Liquid Crystals
Publication details, including instructions for authors and subscription information:
http://www.informaworld.com/smpp/title~content=t713926090

Structure and kinetics of ferroelectric smectic nuclei at the chiral nematic-smectic C* phase transition under the influence of electric fields

W. Haase[a]; S. A. Pikin[ab]; L. A. Beresnev[ab]; S. Hiller[a]
[a] Institut für physikalische Chemie, Technische Hochschule Darmstadt, Darmstadt, Germany [b] Inst. of Crystallography, Russ. Acad. Sci., Moscow, Russia

To cite this Article Haase, W. , Pikin, S. A. , Beresnev, L. A. and Hiller, S.(1993) 'Structure and kinetics of ferroelectric smectic nuclei at the chiral nematic-smectic C* phase transition under the influence of electric fields', Liquid Crystals, 15: 6, 779 — 785
To link to this Article: DOI: 10.1080/02678299308036498
URL: http://dx.doi.org/10.1080/02678299308036498

LIQUID CRYSTALS, 1993, VOL. 15, NO. 6, 779–785

Structure and kinetics of ferroelectric smectic nuclei at the chiral nematic–smectic C* phase transition under the influence of electric fields

by W. HAASE*, S. A. PIKIN†, L. A. BERESNEV† and S. HILLER
Institut für physikalische Chemie, Technische Hochschule Darmstadt, Petersenstrasse 20, W-64287 Darmstadt, Germany

(*Received 12 May 1993; accepted 27 July 1993*)

In the ferroelectric liquid crystal 3-octyloxy-6-[2-fluoro-4-(2-fluoro-octyloxy)phenyl]pyridine (FFP), having the transition smectic C* (S_C^*)–chiral nematic (N*), the formation of the induced S_C^* phase under external electric fields was investigated. In the N* phase, close to the transition temperature $T_{S_C^*N^*}$, the induction of a strongly twisted S_C^* phase is possible. In the case of AC voltage, the growth of nuclei of the S_C^* phase can occur through the formation of circular smectic layers. Dependent on the frequency and amplitude of the electric field, the S_C^* helix within the circles can be twisted or untwisted. This leads to different resulting colours of the circles due to the different anisotropies of the average refractive index and their wavelength dispersion. The coexistence of twisted and untwisted smectic circular nuclei with the supertwisted nematic phase looks like a flower garden ('Darmstädter Blumengarten').

1. Introduction

Because of the intrinsic change in the spontaneous polarization ΔP_S at the transition $T_{S_C^*N^*}$, it is possible to induce the ferroelectric smectic C* phase (S_C^*) in the chiral nematic phase (N*) [1] at slightly above the temperature of the transition $S_C^*N^*$.

The formation of smectic layers, with the direction of the layer surfaces depending on the electric field polarity, was observed [1]. When this occurs, the molecular long axes (director) conserve their N* phase orientation (along the rubbing direction) during the induction of the S_C^* phase, displaying the stronger anchoring of the director with the electrode surfaces, in comparison with the anchoring of the smectic layers. Thus a smectic layer switching with change of polarity takes place. Here we give evidence of new possible structures of the induced S_C^* phase in the case a large change in the spontaneous polarization $\Delta P_S \sim 100\,\mathrm{nC\,cm^{-2}}$ and a small pitch of the helix, $p_0 < 0{\cdot}4\,\mu\mathrm{m}$, in the S_C^* phase.

2. Samples and experiment

We used the ferroelectric liquid crystal FFP, (E. Merck, Darmstadt) having the chemical structure and phase sequence shown in figure 1.

Appreciable changes in the spontaneous polarization, $\Delta P_S \approx 100\,\mathrm{nC\,cm^{-2}}$, and the tilt angle, $\Delta\Theta \approx 30°$, take place at the transition S_C^*–N* (see figure 2).

*Author for correspondence.
†Permanent address: Inst. of Crystallography, Russ. Acad. Sci., Leninskii prosp. 59, 117333 Moscow, Russia.

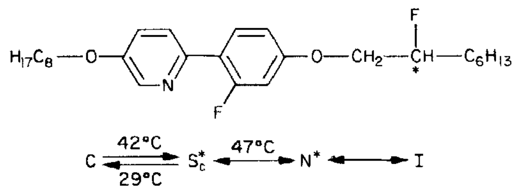

Figure 1. 3-Octyloxy-6-[2-fluoro-4-(2-fluoro-octyloxy)phenyl]pyridine (FFP) and the corresponding phase transition temperatures.

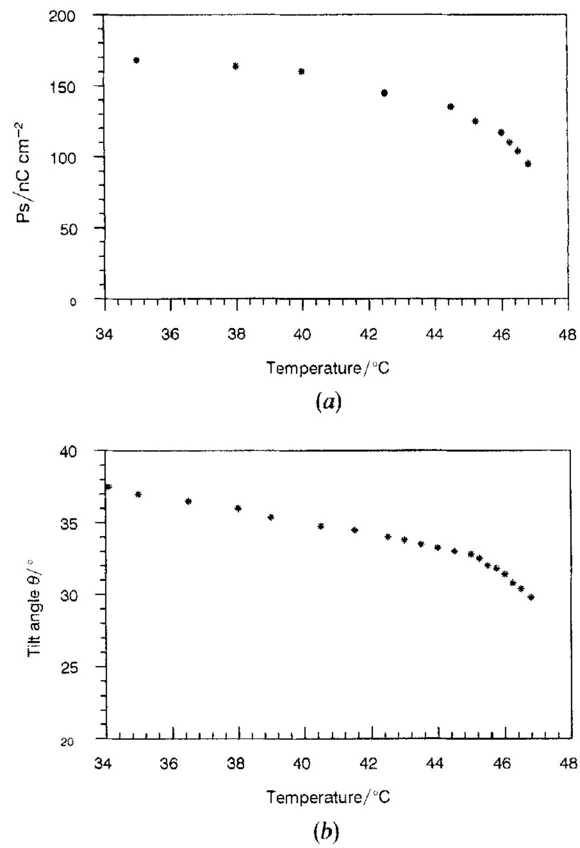

Figure 2. The temperature dependencies of the spontaneous polarization (*a*) and of the tilt angle (*b*) for ferroelectric liquid crystal FFP.

For the electro-optical investigations, a Philips frequency generator and an oscilloscope were connected to our polarizing microscope (Leitz). A high resolution CCD camera (Panasonic) was also attached to the microscope. The results were stored on videotape and printed out using a Sony video printer.

3. Results

Applying a DC voltage or very low frequency (0·1 Hz) AC voltage, we observed the smectic layer switching without the director switching if the temperature interval $\Delta T = T - T_{S_C^*N^*}$ is big enough ($>0{\cdot}15$ K), in accordance with Andersson *et al.* [1]. If ΔT becomes smaller ($<0{\cdot}1$ K) and the frequency of the applied electric field increases, director switching takes place (see figure 3).

The switchable tilt angle Θ strongly depends in this case on the cell thickness d. For $d = 7{\cdot}7\,\mu m$ we obtained $\Theta = 30°$, for $d = 3{\cdot}0\,\mu m$ $\Theta \approx 20°$, and for $d = 0{\cdot}76\,\mu m$ $\Theta \approx 10°$.

Being in the N* phase very close to the S_C^* phase, it is possible to induce the helical S_C^* phase. Increasing the DC voltage leads to a further growth of nuclei of S_C^* phase and unwinding of the helix (see figure 4).

If we apply an AC electric field of moderate strength, (for example, square wave $\pm 9{\cdot}7$ V, cell thickness $d = 7{\cdot}7\,\mu m$), the structure of the induced smectic C* phase depends strongly on the frequency ω. In figure 5 is shown the transformation of the simple focal conic texture (presented in figure 4) into a new organization of smectic layers, if ω increases. It is seen that a circular arrangement of smectic layers with strong defects in the centres of the circles is formed. If the frequency does not exceed some critical value, (for example, $\omega < 200$ Hz; see figure 5 (*d*)), the director in the circles switches totally. This situation can be described by means of the model presented in figure 6 (*a*). At higher frequencies (>350 Hz, see figures 5 (*e*) and (*f*), or at lower amplitudes of the AC voltage, twisting of the director along the z axes and formation of the helical structure within the circles takes place (see figure 6 (*b*)).

Untwisted and twisted circles have different colours and sizes (see figures 5 (*c*), (*d*) and (*f*)). The colour difference is related to the differences in anisotropies of the average refractive index and their wavelength dispersion [2, 3] for untwisted and twisted states. If the frequency increases further, the nematic phase (planar and supertwisted with the cholesteric pitch $p_C \approx 0{\cdot}7\,\mu m$ near $T_{S_C^*N^*}$) appears and its colour differs from that of both S_C^* states mentioned above. The coexistence of the untwisted and twisted smectic C* circles with the nematic areas, having different Cano–Grandjean zones [4] (areas with different numbers of helical twisting turns), looks very beautiful like a flower garden (we have called this texture the 'Darmstädter Blumengarten' [5]; see figure 5 (*g*)).

4. Discussion

In general, the switching on of the external electric field E could be considered as equivalent to a supercooling of the nematic phase, with the extent of supercooling $\Delta T(E)$ proportional to E [1]. The formation of ferroelectric smectic nuclei is possible in such a metastable chiral nematic. If the cell thickness is smaller than the thermodynamically determined critical size of the nuclei, R_C, one can consider the formation of cylindrical nuclei (see figure 7), with the probability $f_0(R)\delta R$ [6, 7] derived from

$$R_C \sim \frac{\alpha T^*(E)}{Q \Delta T(E)}, \qquad (1)$$

Figure 3. The switching of the director in the induced S_C^* phase. $d = 7{\cdot}7\,\mu m$, $\Delta T = 0{\cdot}1$ K, 7 Hz. (*a*) $+9{\cdot}7$ V, (*b*) 0 V (switching the polarity), (*c*) $-9{\cdot}7$ V.

Figure 4. Inducing the helical S_C^* phase under constant electric field close to the transition temperature $T_{S_C^*N^*}$. $\Delta T = 0{\cdot}02$ K, $d = 3{\cdot}0\,\mu m$. (*a*) 2·0 V; (*b*) 2·2 V. Yellow, twisted S_C^* phase; red, untwisted S_C^* phase; blue, nematic phase (planar and supertwisted).

Figure 5. Formation of circular smectic nuclei ('flowers') in the induced S_C^* phase versus frequency of the electric field. $d = 7{\cdot}7\,\mu m$, $\Delta T = 0{\cdot}1$ K. (*a*) 25 Hz, focal conic texture; (*b*) 54 Hz, appearance of the first circular S_C^* nuclei; (*c*) 100 Hz; (*d*) 200 Hz, decrease of nuclei size; (*e*) 350 Hz, coexistence of untwisted (green) and twisted (red) nuclei; (*f*) 500 Hz, twisted S_C^* nuclei (red); (*g*) 550 Hz, $\Delta T = 0{\cdot}15$ K, coexistence of twisted and untwisted S_C^* circles ('flowers') with the nematic phase. (Darmstädter Blumengarten).

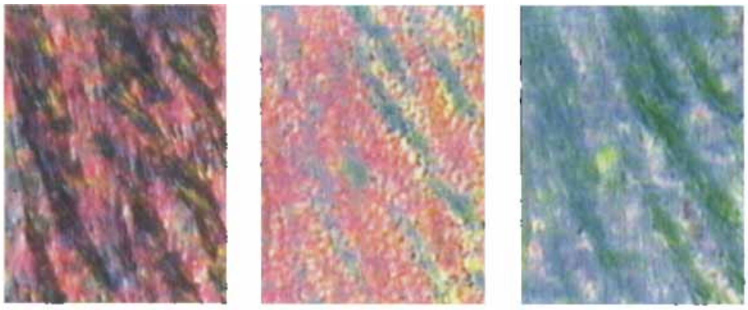

(a) (b) (c)

Figure 3.

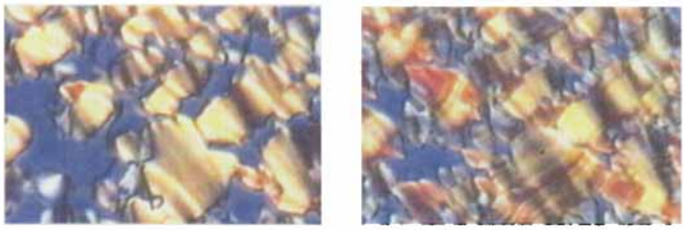

(a) (b)

Figure 4.

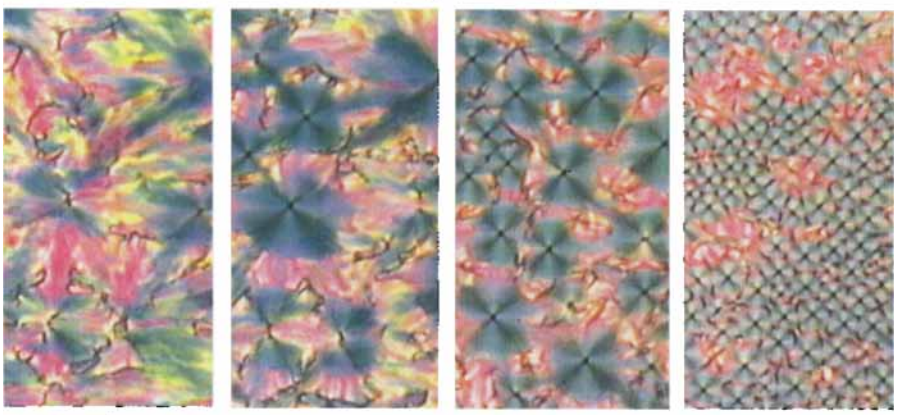

(a) (b) (c) (d)

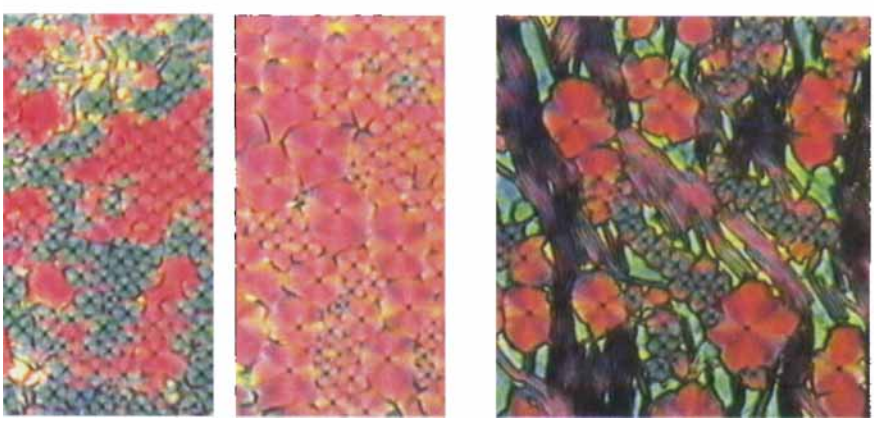

(e) (f) 20 μm (g)

Figure 5.

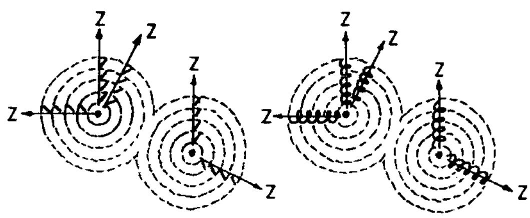

(*a*) (*b*)

Figure 6. Circular organization of smectic layers in nuclei of the induced S_C^* phase in untwisted (*a*) and twisted (*b*) cases. (*a*) corresponds to figures 5(*c*) and (*d*), and (*b*) corresponds to figure 5(*f*).

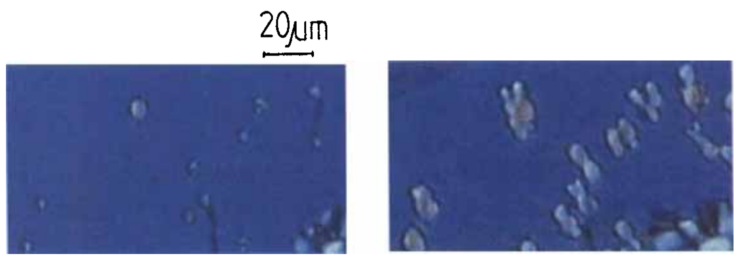

(*a*) (*b*)

Figure 7. Circular S_C^* nuclei growing in the nematic phase ((*a*) = 2·0 V) under an electric field, and further growth and coalescence of the S_C^* nuclei ((*b*) = 2·2 V). $d = 3\,\mu$m, $T - T_{S_C^*N^*} = 0{\cdot}2$ K.

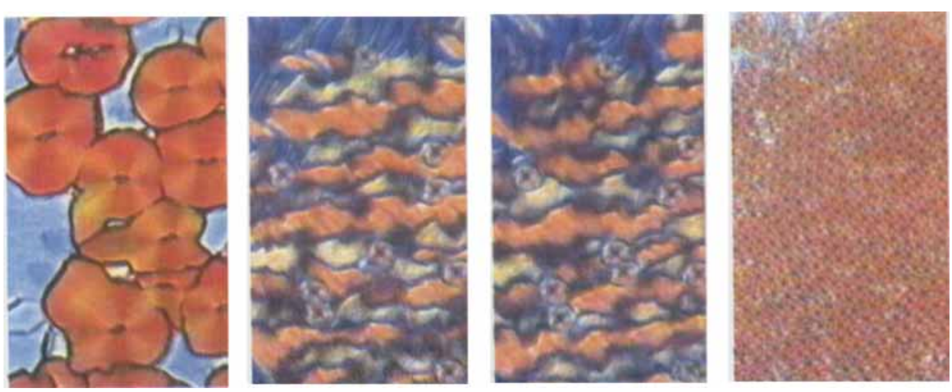

(*a*) 20μm (*b*) (*c*) (*d*)

Figure 8. Dependence of the size of S_C^* nuclei on cell thickness *d*. (*a*) $d = 7{\cdot}7\,\mu$m, $\omega = 1$ kHz; (*b*), (*c*) and (*d*) $d = 3{\cdot}0\,\mu$m. (*b*) and (*c*) The process of diffusion and coalescence of pairs of S_C^* nuclei, 500 Hz; (*d*) Decrease of nuclei size and formation of dense packing with increase in frequency, 1·7 kHz. All the pictures are on the same scale.

$$f_0(R) \sim \exp\left[-\frac{\pi \alpha d R}{T}\left(1-\left(\frac{R}{R_C}-1\right)^2\right)\right], \tag{2}$$

where $T^*(E) = T_{S_C^*N^*} + \Delta T(E)$, α is the surface tension at the surface of separation of two phases and Q is the latent heat of the S_C^*–N^* phase transition. It is seen from (1) and (2) that the value of R_C can be controlled by means of the change in ΔT due to the field E. In particular, if the magnitudes E and ΔT are big enough, the critical radius can be smaller than the cell thickness and the S_C^* nuclei would be of spherical shape.

The rate of size growth of the nuclei with the time dR/dt, at above-critical conditions, also can be evaluated in the framework of classical theory of nuclei growth [7]. Nuclei with sizes smaller than critical must disappear, but the nuclei $R > R_C$ must grow, the 'kinetic' size distribution function $f(R, t)$ being dependent on time. In fact, we are dealing with a heat diffusion controlled growth of nuclei and the rate dR/dt is

$$\frac{dR}{dt} \approx \frac{\kappa \Delta T (R - R_C)}{Q R^2}, \tag{3}$$

where κ is the thermal conductivity.

For an appreciable DC external voltage, very fast movement of the boundary of separation of S_C^* and N^* phases is observed. In this case the density of arising S_C^* nuclei, their growth and diffusion, disappearance and coalescence depend strongly on the surface tension α, cell thickness d and extent of supercooling ΔT (or E).

To slow down these processes and to observe the behaviour of individual nuclei, an alternating electric field should be applied. At sufficiently high frequencies one can artificially stop the relatively slow growth of nuclei at a certain stage, when the nuclei reach a certain size in accordance with the degree of supercooling, but they have no possibility for further growth because of the field switch off (change of polarity).

In figure 8 we present a set of nuclei whose radii depend on the cell thickness (see figures 8 (*a*) and (*b*)) and on the frequency (see figures 8 (*b*) and (*d*)). The sizes of the nuclei are appreciably larger at larger cell thicknesses because supercooling is less. Nuclei of very small radius $\approx$ 2–3 μm could be observed in a very thin cell ($d = 0{\cdot}76\,\mu$m). The diffusion and coalescence of the individual nuclei can also be observed (see figures 8 (*b*) and (*c*)).

It should be noted that the round shape of nuclei is reasonable from the point of view of the minimum surface tension when a smectic grows inside a nematic. Molecules form circular smectic monolayers one after another. There is melted smectic in the circle centre, because of large elastic stresses, and one can observe this defect in the smectic structure as a black spot at the centre of the coloured circles (see figures 5 (*c*)–(*f*)).

One should make a remark here concerning the behaviour of the helix in alternating electric fields. In general, for helix unwinding, the critical amplitude values E_C of the AC field increase with increasing frequency ω. Correspondingly, the change in the transition temperature $T_{S_C^*N^*}$ with increase in E differs from that at $\omega = 0$. This difference is qualitatively shown in figure 9 for frequencies $\omega = 0$, $\omega = \omega_1$ and $\omega = \omega_2 > \omega_1$.

Using the $T^*(E)$ diagrams shown in figure 9 for different frequencies and for the case of smaller polar interactions of the ferroelectric liquid crystal with the surface of the electrodes compared to van der Waals interactions, we can obtain relatively good information [8] about the degree of nematic supercooling ΔT under various conditions. These diagrams (T^*, E^*) allow us to analyse the nuclei kinetics at different

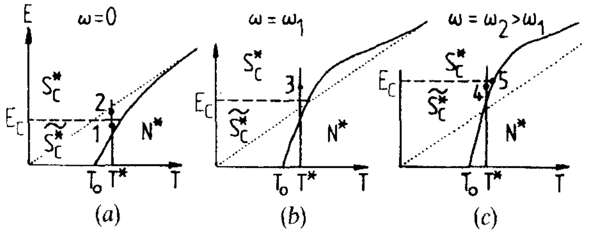

Figure 9. Phase diagrams (E, T) of the transitions between chiral nematic N*, induced twisted smectic C* ($\tilde{S}_C^*$) and untwisted smectic C* phases dependent on frequency of the electric field. T_0, temperature of phase transition S_C^*–N* without electric field; T^*, the temperature of the experiment; E_C, threshold voltage of untwisting of the S_C^* helix.

stages. The case shown in figure 9(*a*) displays the induced twisted S_C^* phase under constant electric field (point 1), which corresponds to the picture in figure 4(*a*). A further increase in the DC field leads to unwinding of the S_C^* helix (point 2 and figure 4(*b*), respectively).

In an AC electric field, the amplitude of the critical field for inducing the S_C^* phase increases. The threshold field E_C of unwinding of the S_C^* helix also increases. Point 3 in figure 9(*b*) corresponds to the untwisted circles in figure 5(*c*) and (*d*) ($\omega = 100$–200 Hz, $\pm 9{\cdot}7$ V). At the same amplitude of the AC voltage, we obtain the twisted induced S_C^* phase, if the frequency ω increases (point 4 in figure 9(*c*)), because of increase in the threshold untwisting field E_C. This case corresponds to figure 5(*f*) ($\omega = 500$ Hz). Finally, at some critical point 5 (figure 9(*c*)), coexistence of twisted and untwisted S_C^* states, together with chiral nematic phase, is possible. The corresponding case is presented in figure 5(*g*).

More detail about the theoretical approach to the thermodynamics and kinetics of the chiral nematic–ferroelectric smectic C* phase transition will be presented [8] in a further publication where we shall also discuss the influence of the cell thickness d on the transition temperature, the diffusion processes of the nuclei and the melting of the S_C^* phase after switching off the electric field.

L.A.B. and S.A.P. are grateful to the Deutsche Forschungsgemeinschaft for personal support.

References

[1] Andersson, G., Flatischler, K., Komitov, L., Lagerwall, S. T., Skarp, K., and Stebler, B., 1991, *Ferroelectrics*, **113**, 361.

[2] Beresnev, L. A., Blinov, L. M., and Dergachev, D. I., 1988, *Ferroelectrics*, **85**, 173.

[3] Abdulhalim, I., and Moddel, G., 1991, *Molec. Crystals liq. Crystals*, **200**, 79.

[4] Cano, R., 1968, *Bull. Soc. fr. Minér. Cristallogr.*, **91**, 20; Grandjean, F., 1921, *C. r. hebd. Séanc. Acad. Sci., Paris*, **172**, 71.

[5] Hiller, S., Beresnev, L. A., Pikin, S. A., Wrobel, S., Pfeiffer, M., and Haase, W., 1993, *22. Freiburger Arbeitstagung Flüssigkristalle*, p. 33.

[6] Pikin, S. A., Beresnev, L. A., Hiller, S., and Haase, W., 1993, *22. Freiburger Arbeitstagung Flüssigkristalle*, p. 47.

[7] Lifshitz, E. M., and Pitaevskii, L. P., 1981, *Course of Theoretical Physics*, Vol. 10 (Pergamon Press).

[8] Pikin, S. A., Beresnev, L. A., Hiller, S., and Haase, W., *Ferroelectrics* (to be published).